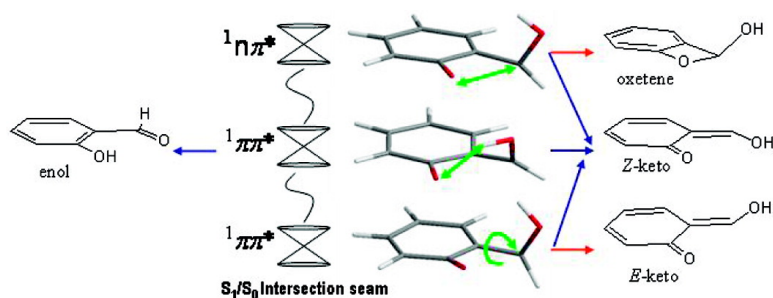


An Extended Conical Intersection Seam Associated with a Manifold of Decay Paths: Excited-State Intramolecular Proton Transfer in *O*-Hydroxybenzaldehyde

Annapaola Migani, Lluís Blancafort, Michael A. Robb, and Anthony D. DeBellis

J. Am. Chem. Soc., **2008**, 130 (22), 6932-6933 • DOI: 10.1021/ja8013924 • Publication Date (Web): 13 May 2008

Downloaded from <http://pubs.acs.org> on February 8, 2009



More About This Article

Additional resources and features associated with this article are available within the HTML version:

- Supporting Information
- Links to the 1 articles that cite this article, as of the time of this article download
- Access to high resolution figures
- Links to articles and content related to this article
- Copyright permission to reproduce figures and/or text from this article

[View the Full Text HTML](#)

An Extended Conical Intersection Seam Associated with a Manifold of Decay Paths: Excited-State Intramolecular Proton Transfer in *O*-Hydroxybenzaldehyde

Annapaola Migani,^{*,†} Lluís Blancafort,[†] Michael A. Robb,[‡] and Anthony D. DeBellis[§]

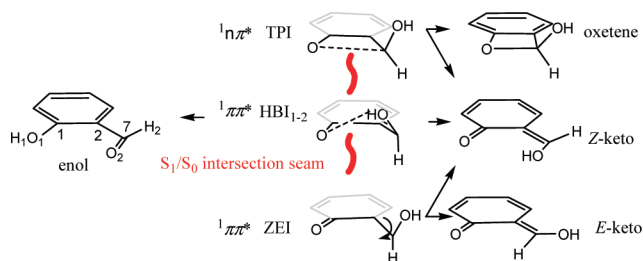
Institut de Química Computacional, Departament de Química, Universitat de Girona, 17071 Girona, Spain, Department of Chemistry, Imperial College London, South Kensington Campus, London SW7 2AZ, U.K., and Ciba Specialty Chemicals, Coating Effects Research Department, 540 White Plains Road, Tarrytown, New York 10591

Received February 25, 2008; E-mail: amigani@stark.udg.edu

O-Hydroxybenzaldehyde (OHBA) is a prototypical photoprotector exhibiting excited-state intramolecular proton transfer (ESIPT).¹ Here we report how its photostability depends on an extended conical intersection seam associated with a manifold of decay paths. Thus, the photoreactivity of OHBA derives from a flat excited-state potential energy surface with barriers of only tenths of electronvolts between the reactant and several conical intersection structures that lead to different products (Scheme 1): two isomers of a hydrogen-bonded intersection (HBI₁₋₂) that lead back to the enol reactant or to the tautomerized keto form in its *Z* conformation; an intersection (ZEI) that mediates the *Z*–*E* isomerization of the keto tautomer; and a twisted-pyramidalized one (TPI) that leads to an oxetene adduct. The intersection structures are connected to each other, forming a continuous seam, and the competition between the products depends on where the seam is accessed after the initial excitation. The overall picture must be also valid for the methyl salicylate (MS) and salicylic acid (SA) analogues of OHBA since it reflects the characteristics reported previously for MS² and SA.³

Femtosecond resolved photoelectron spectroscopy experiments on OHBA find that the proton transfer and internal conversion are decoupled and occur with different time scales.¹ While the proton transfer is complete in approximately 50 fs, the internal conversion rate is temperature and excitation wavelength dependent, with time constants of several picoseconds.^{1,4} Experiments on an OHBA analogue with a locked C₂–C₇ bond suggest that the internal conversion depends on out-of-plane modes.⁵ Consistent with this, previous calculations on OHBA,^{6,7} MS,² and SA³ predict a barrierless planar proton transfer coordinate on the ¹ππ* state, and that the degeneracy for radiationless S₁→S₀ decay is reached along twisting and pyramidalization modes.^{2,3} While these studies report the optimization of some conical intersection structures, here we provide a complete picture of the excited-state potential energy surface for OHBA that illustrates the competition between the different decay paths. Thus, the ground- and excited-state potential energy surfaces have been characterized with CASSCF (complete active space self-consistent field) optimizations of critical points (minima, transition structures, and conical intersections) and reaction path calculations⁸ based on intrinsic reaction coordinate methodology to connect the minima on S₁ and the intersections. The latter have also been connected to the ground-state products with reaction path calculations. The energies are re-evaluated at the CASPT2 level (complete active space second order perturbation). In general, an active space of 14 electrons in 12 orbitals (OH σ/σ*, O lone pair, and 9 π) and the 6-31G* basis have been used. The CASSCF calculations have been done with Gaussian03⁹ and the CASPT2

Scheme 1



calculations with Molcas5.4.¹⁰ More computational details are given as Supporting Information (SI).

After excitation, the hydrogen transfer on the ¹ππ* state is barrierless and leads from the Franck–Condon (FC) structure to the keto tautomer, K-¹ππ*, a planar minimum with a strong hydrogen bond (O₁–H₁ bond = 1.61 Å) that lies 0.9 eV below the vertical S₁ excitation. At the FC structure, a ¹nπ* state is virtually degenerate with the ¹ππ* state, with a calculated gap of less than 0.1 eV (see SI). It has been suggested that crossing to the ¹nπ* state near the FC region could lower the efficiency of the hydrogen transfer,⁷ but this has not been considered here further.

K-¹ππ* is the hub of the manifold of decay paths. It is the short-lived intermediate detected spectroscopically, and the calculated absorption and emission maxima of 4.1 and 2.1 eV agree well with the experimental values in the gas phase and nonpolar solvents (3.7–3.9 and 2.4–2.5 eV, respectively).^{1,4,11} There is a second S₁ keto minimum with ¹nπ* character, K-¹nπ*, located 0.3 eV above K-¹ππ*. It has a “looser” geometry (O₁–H₁ bond = 2.04 Å), and the C₁–O₁ bond is stretched to 1.37 Å. The barrier between the two S₁ minima is 0.4 eV relative to K-¹ππ*. The ¹nπ* state of the keto tautomer is relevant because the TPI region of the seam is associated with that state.

The competition between the different decay paths is shown in Figure 1, which is a sketch of the surface region formed by the S₁ keto minima and the seam, based on the calculated paths and the mapping of the seam. The coordinate that leads from the minima to the seam is a rotation around the C₂–C₇ bond. This bond is a double bond in the keto tautomer, and rotation leads to ethylenic type intersections.¹² The second relevant coordinate connects the ¹ππ* and ¹nπ* excited-state regions. It is a skeletal rearrangement composed mainly of the C₁–O₁ bond length coordinate.

The favored decay path from K-¹ππ* is provided by two conical intersections, HBI₁ and HBI₂. At these structures, the torsional angle around the C₇–C₂ bond (O₂–C₇–C₂–C₁) is 45–55°. The two isomers have the same electronic structure and differ in the pyramidalization at C₇ (O₂–C₇–H₂–C₂ values reported in Figure

[†] Universitat de Girona.

[‡] Imperial College London.

[§] Ciba Specialty Chemicals.

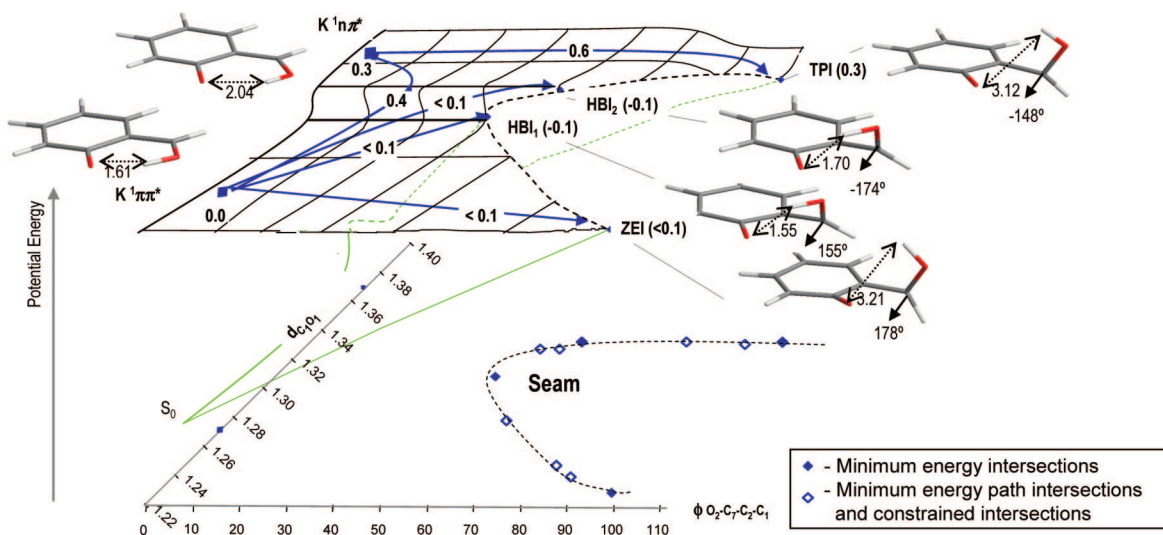


Figure 1. Competing decay paths on the S_1 surface of OHBA. Relative energies of minima, transition structures, and intersections in electronvolts.

1). These structures are analogues of the hydrogen-bonded intersection reported recently for a nitroenamine chromophore that shows ESIPT.¹³ This region of the seam explains the photostability of OHBA. Thus, decay at HBI₁ leads directly to the enol reactant, while decay at HBI₂ leads to the *Z* form of the keto tautomer and proceeds without a barrier to the enol. HBI₁ and HBI₂ can be reached from $K^{-1}\pi\pi^*$ with small barriers (<0.1 eV), in agreement with the short-lived fluorescence of this minimum.

Decay at the ZEI and TPI regions requires a higher degree of C_2-C_7 rotation, up to approximately 90° , and breaking of the hydrogen bond. Similar structures have been reported for MS,² SA,³ and malonaldehyde (MA).¹⁴ ZEI is separated from $K^{-1}\pi\pi^*$ by a barrier of less than 0.1 eV.³ Decay at this region may be photoreactive, as both *E* and *Z* isomers of the keto tautomer can be formed and the barrier for thermal *E*→*Z* isomerization is high (1.84 eV). The alternative decay through TPI involves two activated steps, from $K^{-1}\pi\pi^*$ to $K^{-1}n\pi^*$ and from $K^{-1}n\pi^*$ to TPI, with barriers of 0.4 and 0.3 eV, respectively. Decay at TPI can lead to the *Z* keto tautomer or to the oxetene product. In the latter case, the reaction would lead to degradation.

The seam segments between HBI₁, ZEI, and TPI have been mapped with conical intersection optimizations constraining the $O_2-C_7-C_2-C_1$ (HBI₁-ZEI segment) and $O_2-C_7-H_2-C_2$ (HBI₁-TPI segment) coordinates (see SI). A total of 11 intersection structures have been located, including unconstrained and constrained minima and the minimum energy path intersections (points of intersection found along the $K^{-1}\pi\pi^*\rightarrow$ ZEI and $K^{-1}n\pi^*\rightarrow$ TPI minimum energy paths) (see also Figures SI18–SI20 in SI). To show the connectivity, Figure 1 includes a projection of these structures on the C_1-O_1 and $O_2-C_7-C_2-C_1$ coordinates. Moving along the seam from ZEI to HBI and TPI, S_1 becomes more $n\pi^*$ in character because of configuration mixing with the close-lying S_2 state (see Figure SI21 in SI). The S_0 - S_2 minimal energy separation is 1.2 eV at HBI₂. This suggests that, similar to MA,¹⁴ there is a close-lying three-state intersection. The analysis of this intersection and a better mapping of the seam with intrinsic reaction coordinate calculations in the intersection space¹⁵ will be the subject of future work.

Overall, the HBI and ZEI regions of the seam are separated from the $K^{-1}\pi\pi^*$ minimum by barriers of less than 0.1 eV. The calculated values are 0.04, 0.05, and 0.07 eV for the barriers to HBI₁, HBI₂, and ZEI, respectively, and are within the accuracy of our CASPT2//CASSCF approach. There is also good agreement with the barriers

of 0.1⁴ and 0.2 eV¹ fitted to experimental data. The slightly higher experimental barrier could reflect the slowing down of the process by intramolecular vibrational redistribution (IVR) from the skeletal in-plane modes activated during the hydrogen transfer to the out-of-plane twisting modes. Our results also suggest the *E* keto isomer as a possible photoproduct, although the higher degree of twisting required for the isomerization may disfavor the process, as it requires a larger amount of IVR. The formation of oxetene is less probable because of the higher barrier.

Acknowledgment. This project was funded by Ciba Specialty Chemicals (New York) and Project No. CTQ2005-04563 of the Spanish Ministerio de Educación y Ciencia. A.M. acknowledges a fellowship from the Xarxa de I+D+i de Referència de Química Teòrica i Computacional de Catalunya. The research has been carried out using the facilities of the Catalan Centre for Super-computation (CESCA).

Supporting Information Available: Computational details, Cartesian coordinates, and complete refs 9 and 10.

References

- (1) (a) Lochbrunner, S.; Schultz, T.; Schmitt, M.; Shaffer, J. P.; Zgierski, M. Z.; Stolow, A. *J. Chem. Phys.* **2001**, *114*, 2519–2522. (b) Stock, K.; Bizjak, T.; Lochbrunner, S. *Chem. Phys. Lett.* **2002**, *354*, 409–416.
- (2) Coe, J. D.; Levine, B. G.; Martinez, T. J. *J. Phys. Chem. A* **2007**, *111*, 11302–11310.
- (3) Sobolewski, A. L.; Domcke, W. *Phys. Chem. Chem. Phys.* **2006**, *8*, 3410–3417.
- (4) Nagaoka, S.; Hirota, N.; Sumitani, M.; Yoshihara, K. *J. Am. Chem. Soc.* **1983**, *105*, 4220–4226.
- (5) Nagaoka, S.; Hirota, N.; Sumitani, M.; Yoshihara, K.; Lipczynska-Kochany, E.; Iwamura, H. *J. Am. Chem. Soc.* **1984**, *106*, 6913–6916.
- (6) (a) Sobolewski, A. L.; Domcke, W. *Phys. Chem. Chem. Phys.* **1999**, *1*, 3065–3072. (b) Doltsinis, N. L. *Mol. Phys.* **2004**, *102*, 499–506.
- (7) Coe, J. D.; Martinez, T. J. *Mol. Phys.* **2008**, *106*, 537–545.
- (8) Migani, A.; Olivucci, M. Conical Intersections and Organic Reaction Mechanisms. In *Conical Intersections: Electronic Structure, Dynamics and Spectroscopy*; Domcke, W., Yarkony, D., Köppel, H., Eds.; World Scientific: River Edge, NJ, 2004; Vol. 15.
- (9) Frisch, M. J.; *Gaussian03*, revision B.02; Gaussian, Inc.: Pittsburgh, PA, 2003.
- (10) Andersson, K.; *Molcas*, version 5.4; University of Lund: Sweden, 2003.
- (11) (a) Catalan, J.; Toribio, F.; Acuna, A. U. *J. Phys. Chem.* **1982**, *86*, 303–306. (b) Morgan, M. A.; Orton, E.; Pimentel, G. C. *J. Phys. Chem.* **1990**, *94*, 7927–7935.
- (12) Freund, L.; Klessinger, M. *Int. J. Quantum Chem.* **1998**, *70*, 1023–1028.
- (13) Migani, A.; Bearpark, M. J.; Olivucci, M.; Robb, M. A. *J. Am. Chem. Soc.* **2007**, *129*, 3703–3713.
- (14) Coe, J. D.; Martinez, T. J. *J. Am. Chem. Soc.* **2005**, *127*, 4560–4561.
- (15) Sicilia, F.; Blancafort, L.; Bearpark, M. J.; Robb, M. A. *J. Chem. Theory Comput.* **2008**, *4*, 257–266.

JA8013924